The black-hole candidate GRO J0422+32: MeV emission measured with COMPTEL

van Dijk, R.; Bennett, K.; Bloemen, H.; Collmar, W.; Diehl, R.; Hanlon, L.; Hermsen, W.; Lichti, G.G.; McConnell, M.; Ryan, J.; Schoenfelder, V.; Strong, A.; van Paradijs, J.A.; Winkler, C.

Publication date
1995

Published in
Astronomy & Astrophysics

Citation for published version (APA):
van Dijk, R., Bennett, K., Bloemen, H., Collmar, W., Diehl, R., Hanlon, L., Hermsen, W., Lichti, G. G., McConnell, M., Ryan, J., Schoenfelder, V., Strong, A., van Paradijs, J. A., & Winkler, C. (1995). The black-hole candidate GRO J0422+32: MeV emission measured with COMPTEL. *Astronomy & Astrophysics*, *296*, L33-36.

Astron. Astrophys. 296, L33–L36 (1995)

ASTRONOMY
AND
ASTROPHYSICS

Letter to the Editor

The black-hole candidate GRO J0422+32: MeV emission measured with COMPTEL

R. van Dijk[2,4], K. Bennett[4], W. Collmar[1], R. Diehl[1], W. Hermsen[2], G.G. Lichti[1], M. McConnell[3], J. Ryan[3], V. Schönfelder[1], A. Strong[1], J. van Paradijs[4], and C. Winkler[5]

[1] Max-Planck-Institut für Extraterrestrische Physik, P.O. Box 1603, D-85740 Garching, Germany
[2] SRON-Utrecht, Sorbonnelaan 2, 3584 CA Utrecht, The Netherlands
[3] Space Science Center, University of New Hampshire, Durham, NH 03824, USA
[4] Astronomical Institute, University of Amsterdam, Kruislaan 403, 1098 SJ Amsterdam, The Netherlands
[5] Astrophysics Division, ESTEC, 2200 AG Noordwijk, The Netherlands

Received 23 December 1994 / Accepted 14 February 1995

Abstract. On Aug. 5, 1992, BATSE detected the bright soft X-ray transient GRO J0422+32, also known as Nova Per 1992. The COMPTEL instrument (0.75-30 MeV) aboard the Compton Gamma-Ray Observatory (CGRO) observed this black-hole candidate twice. During the first observation, which started when the X-ray flux was at its maximum, GRO J0422+32 was detected between 1 and 2 MeV. The flux in this energy range was higher than expected from an extrapolation of the standard Sunyaev-Titarchuk Comptonisation model fits to the contemporaneous OSSE and SIGMA data. We discuss several models that may explain the total hard-X/γ-ray spectrum, including the generalised Comptonisation model from Titarchuk. During the second observation, 3 weeks later, no evidence for emission above 1 MeV was seen.

Key words: Gamma rays: observations – Black-hole physics – binaries: general

1. Introduction

The history of the galactic black-hole candidates (BHCs) started with the discovery of the radio-counterpart of the variable X-ray source Cyg X-1 (Braes & Miley 1971). This resulted in the association of Cyg X-1 with the optical counterpart HD 226868 and the subsequent determination of the dynamical parameters of the high-mass X-ray binary (Wade & Hjellming 1972; Webster & Murdin 1972; Bolton 1972). From the mass function, the mass of the compact object in Cyg X-1 was found to be greater than ~ 3 M$_\odot$, larger than the theoretical upper limit for neutron stars. The compact object in Cyg X-1 was thus inferred to be a black hole.

Currently, the group of BHCs consists of six binary systems for which the mass function indicates a compact object with a mass larger than 3 M$_\odot$ (the 'strong' candidates), and of sources which are believed to harbour black holes on the basis of their temporal and spectral signatures (the 'weak' candidates). Mass functions exist for Cyg X-1 (Dolan 1992), LMC X-1 (Hutchings et al. 1987), LMC X-3 (Cowley et al. 1983; Kuiper et al. 1988), A0620-00 (Haswell & Shafter 1990), Nova Muscae 1991=GS1124-683 (Remillard et al. 1992) and V404 Cygni=GS2023+338 (Casares et al. 1992). The first three are high-mass X-ray binaries in which the secondary is a main-sequence or evolved OB star. The last three are soft X-ray transients, a sub-class of the low-mass X-ray binaries. They are usually undetectable in the X- and γ-rays until they suddenly flare up, reaching maximum X-ray brightness within a few days, thereafter decaying over a period of months into undetectability.

One of the spectral signatures which are believed to be characteristic of a black-hole system, is a hard power-law like tail extending well beyond 100 keV with an index $\alpha \lesssim 2$ in the differential $E^{-\alpha}$ energy spectrum (Liang 1993). It might be premature, however, to conclude that neutron-star binaries in general cannot exhibit hard tails beyond 200 keV in their spectra: observations with SIGMA revealed hard X-ray tails up to $\sim 100-200$ keV in the spectra of 3 low-intensity X-ray bursters (Barret & Vedrenne 1994). This was supported by an analysis of a sample of low-mass X-ray binaries, harbouring neutron stars, in the HEAO-A4 catalogue, which shows that the 20-80 keV spectra of these systems become harder as the X-ray luminosity decreases (van Paradijs & van der Klis 1994).

GRO J0422+32 was discovered on Aug. 5, 1992 with the Burst and Transient Source Experiment (BATSE) aboard the Compton Gamma-Ray Observatory (CGRO). The intensity in the $20-300$ keV range increased within a few days to ~ 3 Crab, remaining at that level for three days (Harmon et al. 1992). Hereafter, the intensity of GRO J0422+32 decreased exponentially with a decay time of ~ 41 days (Vikhlinin et al. 1992). The source showed strong variability on all time scales and was seen up to ~ 600 keV with OSSE and SIGMA. The early OSSE data are well represented by a two-component Comptonisation model with temperatures kT of 30 keV and 60 keV and optical depths τ of 6 and 3, respectively (Cameron et al. 1992). For the SIGMA data, a one-component fit gives $kT = 58$ keV and $\tau = 1.99$ (Roques et al. 1994).

The high-energy emission of GRO J0422+32 up to 2 MeV

Send offprint requests to: R. van Dijk (vandijk@sron.ruu.nl) (this paper) and the similarity of the outburst characteristics to BHCs such as A0620-00 and GS2023+338, suggest that GRO J0422+32 is also a BHC (Liang 1993). Kato et al. (1993), assuming that the observed optical modulation is caused by superhumps, derive a mass for the compact object in the range 2.9 $M_\odot - 6.2\ M_\odot$. This is not inconsistent with the mass function derived from recent photometric and spectroscopic measurements (Orosz & Bailyn 1994), implying a mass $\geq 2\ M_\odot$.

2. Instrument and Data Analysis

COMPTEL is one of four instruments aboard CGRO which was launched in April 1991. It is sensitive in the 0.75-30 MeV energy range, thereby forming a link between the hard X-rays/low-energy γ-rays (measured with OSSE and BATSE aboard CGRO) and the $>$ 30 MeV γ-rays (measured with EGRET, also aboard CGRO). COMPTEL is a wide field-of-view imaging instrument (1 steradian) with a positional accuracy of typically 1° and an energy resolution of 8.2% FWHM at 1.5 MeV. The detection mechanism is based on Compton scattering, the dominant photon-matter interaction mechanism in this energy range. For a complete description of the instrument the reader is referred to Schönfelder et al. (1993).

The fluxes and significances reported in this article were determined using a maximum-likelihood ratio (ML) method (de Boer et al. 1992; Bloemen et al. 1994; Schönfelder et al. 1993), for which a background model is required. Lacking an analytical description of the background, the model is presently created from the data itself using a special filter technique. Note that the slight overestimate of source significances that was inherent in the technique described in Bloemen et al. (1994), is now avoided due to an improved algorithm.

The application of the ML method requires the assumption of an *input* spectrum. For the analysis of GRO J0422+32 we used both power-law input spectra with $F \propto E^{-\alpha}$ and Wien input spectra with $F \propto x^2 \exp(-x)$, $x \equiv E/kT$.

3. Observations

COMPTEL observed GRO J0422+32 twice in 1992 (Table 1). The first observation (36.0+36.5) lasted 9 days and covered the plateau-like maximum of the X-ray light-curve just after GRO J0422+32 was discovered (see Harmon et al. 1993). It consists of two parts, which differ by a rotation of the spacecraft around the pointing direction. Obs. 36.0 lasted only 40 hours and was analysed in combination with Obs. 36.5. However, adding Obs. 36.0 reduced the detection significance of GRO J0422+32. It is not yet clear whether this is due to unknown background effects, or time variability of the source. For this reason, Obs. 36.0 was omitted from the analysis presented here. During the second observation (Obs. 39), lasting 16 days, the 20-300 keV flux had decreased to ~ 70% of its maximum value (Harmon et al. 1993).

4. Results

We have detected GRO J0422+32 in Obs. 36.5 in the 1-2 MeV range with a significance of 3.0σ. Fig. 1 shows the location contours obtained with the ML method. In Obs. 39, no emission above 1 MeV is seen, but a weak detection is obtained in the 0.75-1 MeV range. The previously reported ~ 2σ flux point in the 0.75-1 MeV range during Obs. 36.5 (van Dijk et al. 1994) is not confirmed by the improved analysis. We put main emphasis here on the 1-2 MeV result, because it is most important for comparison with models, as discussed in Section 5.

Table 1. List of observations. The 5 columns show: 1) the observation ID in GRO notation; 2) the angular distance of GRO J0422+32 to the pointing direction; 3) the start date and time; 4) the end date and time; 5) the number of days since Aug. 11 (peak X-ray flux).

Obs	Z [°]	Start (1992)	End (1992)	N [days]
36.0	3.91	Aug. 11, 01:59 UT	Aug 12, 18:22 UT	1-2
.5	3.32	Aug. 12, 19:00 UT	Aug 20, 15:28 UT	2-10
39	2.99	Sep. 01, 05:40 UT	Sep 17, 15:17 UT	21-36

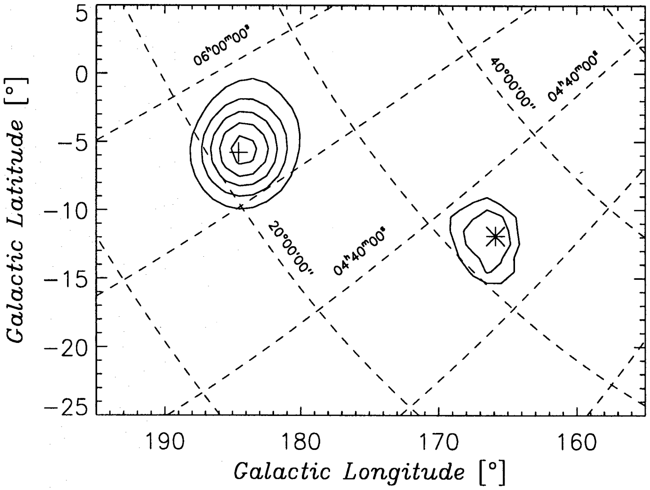

Fig. 1. Skymap in the 1-2 MeV range for Obs. 36.5 showing GRO J0422+32 (∗) and the Crab (+). The contours plotted for GRO J0422+32 are the 95% and 99% error location contours; the contours for the Crab are at arbitrary levels. Note that the quasar PKS 0528+134 reported by Collmar et al. (1993), located only 8° from the Crab, is not detected at these low energies.

Table 2 lists the fluxes with 1σ errors and the 2σ upper limits per observation period for the 0.75-1 and 1-2 MeV ranges. Both a power-law spectrum with index $\alpha = 2$ and Wien spectra with different temperatures kT have been used as input spectra. It is evident from Table 2 that the derived flux values and upper limits are only weakly dependent on the assumed input spectrum. We plotted the COMPTEL 1-2 MeV flux point and the upper limits for the 0.75-1 MeV, 2-3 MeV, 3-10 MeV and 10-30 MeV ranges in Obs. 36.5 in Fig. 2, using a Wien spectrum with $kT = 100$ keV for the lowest two energy ranges and an E^{-2} power-law spectrum for the higher energy ranges.

We have also looked for time variations of the 1-2 MeV flux in Obs. 36.5 by dividing this observation into 7 parts of roughly 1 day duration. Although we obtain a $> 2\sigma$ flux in only two of these time intervals, the results are consistent with a constant flux due to the high upper limits in the other time intervals and the uncertainties associated with the background modelling in sparse dataspaces.

Table 2. The fluxes and 2σ upper limits for the 0.75-1 and 1-2 MeV ranges for Obs. 36.5 and 39. The kT values refer to the temperatures of the Wien input spectra (simulated point-spread functions (PSFs)), the α value refers to the index of the power law input spectrum (modelled PSFs). The errors quoted are 1σ errors.

Obs	E [MeV]	Flux/upper limit [$\mathrm{cm}^{-2}\ \mathrm{s}^{-1}\ \mathrm{MeV}^{-1}$]				
		$kT = 100$ keV	$kT = 120$ keV	$kT = 150$ keV	$kT = 200$ keV	$\alpha = 2$
36.5	0.75-1	$< 1.4 \times 10^{-3}$	$< 1.3 \times 10^{-3}$	$< 1.4 \times 10^{-3}$	$< 1.4 \times 10^{-3}$	$< 0.9 \times 10^{-3}$
	1-2	$(2.8 \pm 1.0)10^{-4}$	$(2.8 \pm 1.0)10^{-4}$	$(2.9 \pm 1.0)10^{-4}$	$(2.9 \pm 1.0)10^{-4}$	$(2.6 \pm 0.8)10^{-4}$
39	0.75-1	$(1.1 \pm 0.4)10^{-3}$	$(1.1 \pm 0.4)10^{-3}$	$(1.1 \pm 0.4)10^{-3}$	$(1.1 \pm 0.4)10^{-3}$	$(0.8 \pm 0.3)10^{-3}$
	1-2	$< 1.5 \times 10^{-4}$	$< 1.5 \times 10^{-4}$	$< 1.5 \times 10^{-4}$	$< 1.4 \times 10^{-4}$	$< 1.2 \times 10^{-4}$

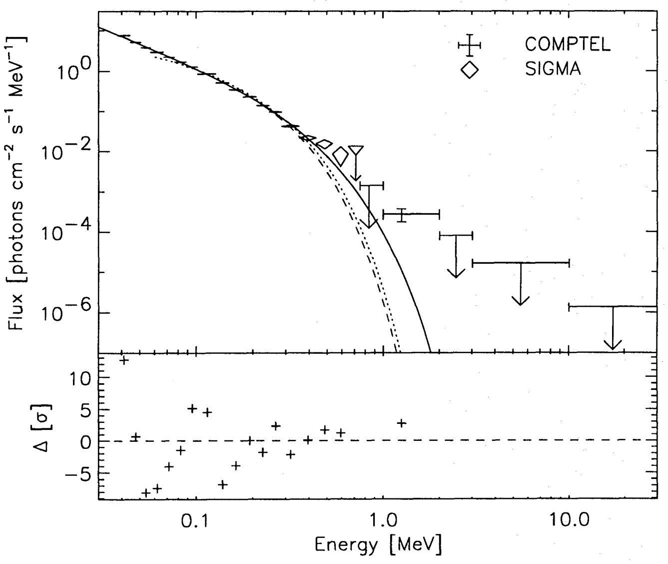

Fig. 2. The COMPTEL 1-2 MeV datapoint and upper limits for Obs. 36.5, together with the SIGMA datapoints. *Dashed line:* extrapolated ST80 fit to SIGMA data (Roques et al. 1994); *dotted line:* extrapolated 2-component ST80 fit to OSSE data (Cameron et al. 1992); *solid line:* extrapolated fit B from Table 3. The lower plot region shows the differences between fit B and the SIGMA and COMPTEL datapoints.

Table 3. Results of model fitting. *Column 1:* the data used with S denoting SIGMA and C denoting COMPTEL; *column 2:* the Comptonisation model (see discussion); *column 3:* the reduced chi-square value and the number of degrees of freedom; *column 4:* the temperature [keV] and *column 5:* the optical depth. Errors quoted are 1σ errors.

Data	Model	χ^2_ν(dof)	kT	τ	Fit
$S + C$	ST80	27.3(16)	58 ± 1	2.00 ± 0.03	A
$S + C$	T94	27.4(16)	100 ± 4	1.04 ± 0.05	B
$S(> 130\ \mathrm{keV}) + C$	T94	3.05(8)	102 ± 13	1.1 ± 0.3	C

5. Discussion

The 1-2 MeV flux for Obs. 36.5 is somewhat higher than expected from an extrapolation of the Comptonisation model fits (Sunyaev & Titarchuk 1980, hereafter ST80) to the SIGMA and OSSE data, denoted by the dashed and dotted lines in Fig. 2. From a comparison of the number of counts expected for these extrapolated fits and the number of counts observed in the 1-2 MeV range, we derive a significance of 2.8σ for the excess. Such a deviation from the fitted ST80 model at high energies is also observed in the 300-700 keV SIGMA data (Roques et al. 1994), for which an excess of 5.8σ was derived. However, the ST80 Comptonisation model used to fit the SIGMA and OSSE data is known to break down at high plasma temperatures and high photon energies (e.g. Grebenev 1993). Titarchuk (1994, hereafter T94) developed a generalised Comptonisation model which is valid in a much larger region of the (kT, τ) space due to the inclusion of relativistic corrections in the diffusion coefficients of the energy and space operators. We fitted both the ST80 model and the optically thin version of the T94 model to the combined SIGMA and COMPTEL data, the results of which are shown in Table 3. The fit labeled 'A' is equal to the SIGMA fit in Fig. 2 (the dashed line), while fit B is shown as a solid line. Note that the T94 model for these temperatures and optical depths can be approximated in the 1-2 MeV range by a Wien-type spectrum of temperature $kT \approx 100$ keV.

Although the quality of the fits in Table 3 is poor for both models, it is evident that the T94 fits give a significantly higher plasma temperature and smaller optical depth than the ST80 model, just as expected. This is in accordance with the higher temperatures found for Cyg X-1 from COMPTEL observations (McConnell et al. 1994), and from reflection models applied to EXOSAT data (Haardt et al. 1993). It is also clear from Table 3 that the reduced chi-square values are significantly smaller if the lowest SIGMA datapoints are omitted (with no effect on the fitted parameters), indicating a more complicated spectral shape at lower energies.

At higher energies, the fit with the more appropriate T94 model clearly lies above the ST80 model fits (Fig. 2). Even for the T94 model fits, however, the COMPTEL 1-2 MeV datapoint lies 2.7σ above the model value (2.6σ if we account for the decay of the hard X-ray intensity of GRO J0422+32 during the ~ 40 days SIGMA observations). When the high SIGMA datapoints in the 300-700 keV range are taken into account as well, the significance of these high-energy deviations becomes even larger. The 0.75-1 MeV flux measured in Obs. 39.0 is consistent with the T94 model fits presented here.

The question arises as to whether the possible deviations at high energies (> 300 keV) indicate the need for an additional spectral component. Until now, there have been few detections of black-hole candidates (BHCs) above 100 keV and as a consequence, our understanding of these objects at γ-ray energies is far from complete. There are several models that predict enhanced MeV emission from BHCs.

The transient 'γ-ray bump' observed in 1979 in the spectrum of Cyg X-1 (Ling et al. 1987), which was much more pronounced than the excess presented here for GRO J0422+32, has been interpreted as the emergence of a pair-dominated hot thermal cloud in the inner accretion disk region (Liang & Dermer 1988; Liang 1990; Melia & Misra 1993). Such strongly enhanced MeV emission has so far not been seen by the later OSSE and COMPTEL observations of Cyg X-1, although the 100 keV flux was also very low during some of these observations (Leising et al. 1993; McConnell et al. 1994).

Instead of *thermal* pair plasmas, contributions at high energies may also come from *non-thermal* pair plasmas. Jourdain & Roques (1994) modelled the high energy SIGMA data on BHCs with inverse Comptonisation of a dense UV radiation field by a non-thermal pair plasma. The plasma is fuelled by photon-photon interactions of X-ray photons with the high-energy photons of average energy $\sim$ 18 MeV from π^0 decay near the compact object (they do not take into account the influence of π^- and π^+ production). This model, in combination with an ST80 model below $\sim$ 200 keV, can explain the 30-700 keV SIGMA data on GRO J0422+32 and Cyg X-1 quite well (Jourdain & Roques 1994). However, note that the 1-2 MeV flux expected from their fit to the SIGMA data on GRO J0422+32 is a factor 10 higher than measured, which suggests that the size of the interaction region that they derive (100 km) is too large.

Enhanced MeV emission may also be related to the transient line features around 390 keV observed for 1E1740.7-2942 (Cordier et al. 1993) and around 170 keV and 476 keV observed for Nova Muscae 1991 (Sunyaev et al. 1992; Goldwurm et al. 1992). Following the radio observations of jets in 1E1740.7-2942 (Mirabel et al. 1993), Skibo et al. (1994) proposed a model for these lines based on temporarily enhanced jet-like energy release in the form of plasma and hard-spectrum photons up to 10 MeV. The positions of the line features that arise in this model are a function of viewing angle and range up to MeV energies. The $<$ 500 keV line features have also been tentatively identified with the 511 keV electron-positron annihilation line (Sunyaev et al. 1992; Hua & Lingenfelter 1993; Hameury et al. 1994). Yet another explanation for the 476 keV line observed in Nova Muscae 1991 comes from the recent discovery of high ^{7}Li abundances in the BHCs A0620-00 and V404 Cyg (Martin et al. 1994a,b). In this respect, we point out that the possible presence of nuclear line emission in the 1-2 MeV range is still under investigation. Note that the 1-2 MeV detection involves photons with less energy than the 2.2 MeV photons liberated when the neutrons created in the formation of ^{7}Li are captured by protons.

6. Conclusions

The COMPTEL observations of GRO J0422+32, in combination with the SIGMA data, show evidence for possible deviations from the generalised Comptonisation model (Titarchuk 1994) in the energy range from 300 keV up to 2 MeV. It is evident that sensitive future studies in the region around 1 MeV will provide valuable information for our understanding of the mechanisms that play a role in sources like GRO J0422+32.

Acknowledgements. R. van Dijk acknowledges support by the Netherlands Foundation for Research in Astronomy (NFRA) with financial aid from the Netherlands Organisation for Scientific Research (NWO) under contract number 781-71-042. The COMPTEL project is supported by the German government through DARA grant 50 QW 90968, by NASA under contract NAS5-26645, by the Netherlands Organisation for Scientific Research (NWO). We thank J.P. Roques for providing the SIGMA data on GRO J0422+32.

References

Barret D., Vedrenne G., 1994, ApJS 92, 505

Bloemen H. et al., 1994, ApJS 92, 419

Bolton C.T., 1972, Nat 235, 271

Braes L.L.E., Miley G.K., 1971, Nat 232, 246

Cameron R.A. et al., 1992, IAU Circ 5587

Casares J., Charles P.A., Naylor T., 1992, Nat 355, 614

Collmar W. et al., 1993, AIP 280, p483

Cordier R. et al., 1993, A&A 275, L1

Cowley et al., 1983, ApJ 272, 118

de Boer H. et al., 1992, in: Data Analysis in Astronomy IV, eds. V. Di Gesù (New York: Plenum Press), Vol 59, p241

Dolan J.F., 1992, ApJ 384, 249

Goldwurm A. et al., 1992, ApJ 389, L79

Grebenev S. et al., 1993, A&AS 97, 281

Haardt F. et al., 1993, ApJ 411, L95

Hameury J.-M., Marck J.-A., Pelat D., 1994, A&A 287, 795

Harmon B.A. et al., 1992, IAU Circ 5584

Harmon B.A. et al., 1993, AIP 280, p314

Haswell C.A., Shafter A.W., 1990, ApJ 359, L47

Hua X.-M., Lingenfelter R.E., 1993, ApJ 416, L17

Hutchings J.B. et al., 1987, AJ 94, 340

Jourdain E. & Roques J.P., 1994, ApJ 426, L11

Kato T., Mineshige S., Hirata R., 1993, IAU Circ 5704

Kuiper L., van Paradijs J., van der Klis M., 1988, A&A 203, 79

Leising M.D. et al., 1993, IAU Circ 5823

Liang E.P., Dermer C.D., 1988, ApJ 325, L39

Liang E.P., 1990, A&A 227, 447

Liang E.P., 1993, AIP 280, p396

Ling J.C. et al., 1987, ApJ 321, L117

Martin E.L. et al., 1994a, ApJ 435, 791

Martin E.L., Spruit H.C., van Paradijs J., 1994b, A&A 291, L43

McConnell M.L. et al., 1994, ApJ 424, 933

Melia F., Misra R., 1993, ApJ 411, 797

Mirabel I.F. et al., 1993, A&AS 97, 193

Orosz J., Bailyn C., 1994, IAU Circ 6103

Remillard R.A., McClintock J.E., Bailyn C.D., 1992, ApJ 399, L145

Roques J.P. et al., 1994, ApJS 92, 451

Schönfelder et al., 1993, ApJS 86, 657

Skibo J.G., Dermer C.D., Ramaty R., 1994, ApJ 431, L39

Sunyaev R.A., Titarchuk L.G., 1980, A&A 86, 121 (*ST80*)

Sunyaev R. et al., 1992, ApJ 389, L75

Titarchuk L., 1994, ApJ 434, 570 (*T94*)

van Dijk R. et al., 1994, AIP 304, p197

van Paradijs J. & van der Klis M., 1994, A&A 281, L17

Vikhlinin A. et al., 1992, IAU Circ 5608

Wade C.M., Hjellming R.M., 1972, Nat 235, 271

Webster B.L., Murdin P., 1972, Nat 235, 37